pH prediction in concentrated aqueous solutions under high pressure of acid gases and high temperature

C. Plennevaux, N. Ferrando, J. Kittel, Marion Fregonese, Bernard Normand,
T. Cassagne, F. Ropital, M. Bonis

pH prediction in concentrated aqueous solutions under high pressure of acid gases and high temperature

C. Plennevaux[a], N. Ferrando[b], J. Kittel[c*], M. Frégonèse[d], B. Normand[d], T. Cassagne[a], F. Ropital[c], M. Bonis[a]

[a] TOTAL, Avenue Larribau, Pau Cedex 64018, France
[b] IFP Energies nouvelles, 1 et 4 avenue de Bois-Préau, 92852 Rueil-Malmaison, France
[c] IFP Energies nouvelles, Rond-point de l'échangeur de Solaize BP3, 69360 Solaize, France
[d] MATEIS, INSA de Lyon, CNRS UMR 5510, Avenue Jean Capelle, Villeurbanne Cedex 69621, France

Abstract

An extended model for pH prediction in oil and gas environments has been developed. Accurate pH calculations for high pressure and high temperature applications depends mainly on CO_2 and H_2S partial pressures, the ionic strength, the chemical composition of the solution, and the temperature. Accounting for the non-ideal behaviors of liquid and gas phases allows pH calculations up to 200 °C, 2000 bar total pressure, and ionic strengths up to 5 mol.L^{-1}. The results are consistent with experimental measurements and with other models reported in the literature.

Keywords: acid solutions, modeling studies, pH, CO_2, H_2S, high pressure, high temperature.

1   Introduction

Corrosion of metallic materials in oil and gas wells is strongly influenced by several parameters, among which carbon dioxide (CO_2) and other corrosive agents as hydrogen sulfide (H_2S) play a central role in controlling the pH. Corrosion prediction models have thus been developed starting several decades ago. While the early model proposed by de Waard and Milliams [1] considered only temperature and CO_2 partial pressure, continuous improvements have been made to take into account a greater number of parameters.

The efforts to propose new more accurate models have been shared by oil companies or research institutions, and there is a large number of open or commercial models. A large variety of prediction strategies is found. A comprehensive review was recently issued by Nesic [2], who proposed to classify oil and gas corrosion models in three categories: i/ empirical models are essentially based on correlations with laboratory or field data [3-6]; ii/ mechanistic models require a strong theoretical background. Most parameters have a clear physical meaning, and such models often combine chemical evaluation of the environment, electrochemical reactions, hydrodynamics and precipitation of corrosion products [1,7-21]. Most of these models are proprietary or commercial; iii/ finally, semi-empirical models lie in-between the two previous categories. They often contain a part of theoretical calculations, completed by empirical functions calibrated with experimental database [22-26]. The

---

model called Corplus (Model A), developed by some of the authors' company, belongs to the semi-empirical type. It is based on a detailed analysis of water chemistry for pH calculation, and a large amount of corrosion field data.

A comparative study of the performances and limitations of a large number of models was proposed by Nyborg in 2010 [27]. It shed the light on strong limitations of most of these models to temperatures below 150 °C and acid gas pressure below 70 bar. These limitations were not a problem for typical oil and gas fields operated from the eighties to 2000. However, the number of high pressure (HP) and high temperature (HT) oil and gas fields has considerably increased in the recent years, which cannot be easily treated with common models based on simple assumptions. Various reasons can be found to explain these limitations, depending on the modeling method. As described in details by Nyborg [27], an accurate corrosion prediction relies on several important factors, including in-situ pH prediction, effect of protective films, effect of oil wetting and connection with fluid flow. Model A was included in the comparative study of Nyborg [27], and is considered to be reliable up to 120 °C and 20 bar CO_2. These limitations are to a great extent associated with the pH prediction tool which is included in the model.

The goal of this work is therefore to describe the methodology used to extend Model A to HP/HT applications and to highly concentrated brines. The evolution of the model comprises two major steps which are described in this paper: i/ a better description of gases solubility, taking into account the fugacity of gaseous components; ii/ an improvement of chemical equilibria description through the calculation of activity coefficients of species in the liquid phase.

It is then compared to experimental data and to other models from the literature.

2 Background

Before presenting the new model in detail, a brief description of the method of pH calculation used in Model A is proposed. Two groups of reactions are considered: i/ dissolution of acid gases in the aqueous liquid phase and ii/ chemical dissociation of weak acid components [28].

The corresponding reactions are described below.

At the liquid/gas interface, a quantity of CO_2 and H_2S dissolves in the aqueous solution according to reactions (1) and (2).

$$CO_{2(g)} \rightleftharpoons CO_{2(aq)} \qquad\qquad S_{CO2} \qquad\qquad (1)$$

$$H_2S_{(g)} \rightleftharpoons H_2S_{(aq)} \qquad\qquad S_{H2S} \qquad\qquad (2)$$

In the liquid phase, dissolved carbon dioxide hydrates to carbonic acid following reaction (3).

$$CO_{2(aq)} + H_2O \rightleftharpoons H_2CO_3 \qquad\qquad K_{hyd} \qquad\qquad (3)$$

Carbonic acid and hydrogen sulfide are weak acids. They are likely to dissociate according to reactions (4) to (7).

$$H_2CO_3 \rightleftharpoons H^+ + HCO_3^- \qquad\qquad K \qquad\qquad (4)$$

$$HCO_3^- \rightleftharpoons H^+ + CO_3^{2-} \qquad\qquad K_2 \qquad\qquad (5)$$

$$H_2S_{(aq)} \rightleftharpoons H^+ + HS^- \qquad\qquad K'_1 \qquad\qquad (6)$$

$$HS^- \rightleftharpoons H^+ + S^{2-} \qquad\qquad K'_2 \qquad\qquad (7)$$

The dissolution of acid gases is described by solubility constants S_{CO2} and S_{H2S} and equilibrium constants K_{hyd}, K, K'_1, K_2 and K'_2 define chemical equilibria in the liquid phase.

Solubility and equilibrium constants depend only on temperature as long as fugacity and activity notions are used. Under ideal conditions, fugacity and activity are equivalent to partial pressure and concentration. However, this assumption cannot be made under high pressure or in highly concentrated solutions. In order to continue to manipulate partial pressures and concentrations, a common practice consists in using apparent solubility and equilibrium constants which include the impact of both the pressure and the ionic strength (I) in addition to the temperature effect. These constants are then expressed as:

$$S_{i,app}(T,P,I) = \frac{c_i}{P_i} \tag{8}$$

$$K_{app}(T,I) = \prod_i (c_i)^{v_i} \tag{9}$$

In these expressions, $S_{i,app}(T,P,I)$ is the apparent solubility constant of H_2S or CO_2 in water, $K_{app}(T,I)$ is the apparent equilibrium constant of any one of the chemical reactions (3) to (7) and P_i, c_i and v_i are respectively the partial pressure of gas i and the concentration and the stoechiometric coefficient of component i in the liquid phase.

This method is acceptable as long as the apparent constants $S_{i,app}$ and K_{app} are accurately calculated at given temperature, ionic strength and pressure. The easiest method consists in using empirical expressions as proposed in [6,29-31].
The main difficulty with this approach is to describe the apparent constants with three different variables. Thus, the validity domain is often limited to low pressures, low temperatures and to slightly concentrated brines solutions. In the case of Model A, the limits are 120 °C, 20 bar of CO_2 and an ionic strength of 0.75 mol.L^{-1}. In order to extend its range of application, the calculation method of equilibrium constants must be reconsidered taking into account the non-ideal behaviors of the gas and liquid phases. This requires more complete thermodynamics, as described in the next section.

3 Evolution of the model for HP/HT conditions

General methodology
At high pressure, the gas phase cannot be considered as ideal and fugacity correction needs to be applied to account for interactions between gas molecules. As a consequence, three corrections must be applied in the solubility calculations leading to the ensemble Henry's law [32-34] (10):

$$\gamma_i \times c_i \times H_i(T) \times \exp\left[\int (v_i^\infty / RT) dP\right] = \Phi_i \times P_i \tag{10}$$

In this expression, c_i is the concentration of component i in the liquid phase, $H_i(T)$ is the Henry's constant characterizing the solubility of gas i in water and P_i is the partial pressure of component i. The activity coefficient γ_i accounts for non-ideality of dissolved gas, the exponential term is known as the Poynting correction [32,33] considering the effect of high pressures on the partial molar volume of the solute under infinite dilution (v_i^∞) and the fugacity coefficient Φ_i corrects the gas phase for non-ideal behavior.

Similarly, reactions in concentrated solutions are influenced by interactions between dissolved molecules and ions. To consider the non-ideal behavior of the liquid phase, the calculation of chemical equilibrium constants must also be corrected adding activity coefficients (11):

$$K(T) = \prod_i (a_i)^{v_i} = \prod_i (\gamma_i \times c_i)^{v_i} \tag{11}$$

In this expression, $K(T)$ is the equilibrium constant of one of the chemical reactions (3) to (7), a_i, c_i and γ_i are respectively the activity, the concentration and the activity coefficient of component i in the liquid phase and v_i is the stoechiometric coefficient of component i for the chemical equilibrium considered.

In order to make the model modification as simple as possible, we simply replaced the empirical expressions of solubility constants and chemical equilibrium constants used in Model A by new expressions derived from (10) and (11), according to respectively (12) and (13):

$$S_{i,app}(T,P,I) = \frac{\Phi_i}{\gamma_i \times H_i(T) \times \exp\left[\int \left(v_i^\infty / RT\right) dP\right]} = \frac{c_i}{P_i} \tag{12}$$

$$K_{app}(T,I) = K(T) \times \prod_i \left(\gamma_i\right)^{-v_i} = \prod_i \left(c_i\right)^{v_i} \tag{13}$$

Determination of true Henry's constants and chemical equilibrium constants

CO_2 and H_2S Henry's constant values used in Equation (12) are determined with the correlation proposed by de Hemptinne et al. as:

$$\ln\left(H_i(T)\right) = A_i + \frac{B_i}{T} + \frac{C_i}{T^2} \tag{14}$$

where $H_i(T)$ is the Henry's constant on the mole fraction scale characterizing the solubility of gas i in water, T is the temperature (K) and A_i, B_i and C_i have the values given in Table 1 [35].

This expression was established from experimental databases covering temperature range from 20 °C to 200 °C.

Chemical equilibrium constants $K(T)$ were also determined from correlations presented in the literature [36-40].

Fugacity coefficients of gaseous components

The Soreide and Whitson [41] modification of the Peng-Robinson equation of state (EOS) [42] is used for describing the fugacity of CO_2, H_2S, H_2O and CH_4 in the gas phase. Thus the effect of high pressure of natural gas on acid gas fugacity is included in the calculations.

The Peng-Robinson EOS (15) is derived from Van der Waals theory:

$$P = \frac{RT}{v-b} - \frac{a(T)}{v(v+b) + b(v-b)} \tag{15}$$

In this expression, the pressure is calculated as a function of a repulsive term taking into account the co-volume b and a parameter a regarded as a measure of intermolecular attraction forces. This parameter depends on temperature. R is the gas constant, T is the temperature (K), P the total pressure (Pa) and v the molar volume (m^3.mol^{-1}).

Peng and Robinson used this equation to express the fugacity coefficient Φ_i of a component i in a mixture [42]:

$$\ln(\Phi_i) = \frac{b_i}{b}(Z-1) - \ln(Z-B) - \frac{A}{2\sqrt{2}B}\left(\frac{2\sum_j x_j a_{ji}}{a} - \frac{b_i}{b}\right)\ln\left(\frac{Z+2.414B}{Z-0.414B}\right) \tag{16}$$

where $A = \dfrac{aP}{R^2 T^2}$, $B = \dfrac{bP}{RT}$ and $Z = \dfrac{Pv}{RT}$

In this expression, x_i is the mole fraction of component i, b_i is the co-volume of component i, a_{ji} characterizes the binary system formed by components j and i. SI units are used in this equation.

The presence of salts in the formation water also has a great influence on gas solubility, which is not directly taken into account by the Peng and Robinson expression. Thus, Soreide and Whitson have proposed an extension of the Peng-Robinson EOS for treating the case of water-hydrocarbon mixtures in the presence of sodium chloride in the water phase. One of the main changes consists in a modification of the attractive term of pure water.

Equation (16) was used in this study for the calculation of gases fugacity coefficients, using constant parameters values from reference [35].

Activity coefficients in the liquid phase

The calculation of activity coefficients of components in the liquid phase was performed applying Pitzer's model [43,44] which derives from Debye-Hückel's method. This activity model is adapted to describe thermodynamic properties of concentrated brines solutions.
Debye-Hückel's equations give an expression of activity coefficients of ionic species from the ionic strength of the solution. This method takes into account long distance interactions between ionic species corresponding to electrostatic interactions. This approach is valid for slightly concentrated solutions (maximum molality of salts of about 1 mol.kg^{-1} of water).
To adapt the activity model to highly concentrated brines, Pitzer has added short distance interaction terms to the Debye-Hückel's model corresponding to interactions between ionic species and the solvent.
The formalism of Pitzer's model will not be detailed in this paper. However, Table 2 summarizes all binary and ternary interaction parameters that we considered in our system, considering dissolved CO_2 and H_2S and the following ionic species: Ca^{2+}, Na^+, Cl^-, H^+, HCO_3^-, CO_3^{2-}, HS^-, S^{2-} and HO^-.

Validity domain, capabilities and limitations of the new model

At the present time, the new model only applies to CO_2, H_2S, CH_4 and H_2O for the gas phase. In the liquid phase, ionic species that are considered for calculations of activity coefficients are Ca^{2+}, Na^+, Cl^-, H^+, HCO_3^-, CO_3^{2-}, HS^-, S^{2-} and HO^-. The main input parameters of the model are: total pressure and partial pressures of CO_2, H_2S and CH_4, temperature and ionic composition of the solution (Ca^{2+}, Na^+, Cl^-, HCO_3^-). The main output data are: in-situ pH, the fugacity of gases, the concentration and the activity of all species in the liquid aqueous phase.
Precipitation of solids is not considered and acetate ions are also not included in the new model. It is a perspective of this work to include acetate anions and iron cations parameters in Pitzer's formulation.

As a first approximation, the validity domain can be estimated from the validity of individual elements used in the new model. The main limitations arise from the validity domains of equilibrium constants and of interaction parameters; we can thus expect good predictions up to 200 °C, 1000 bar total pressure, and ionic strengths up to 5 mol.L^{-1}. However, the availability of experimental data for model validation does not cover this domain completely. A discussion of the validity domain based on comparisons with experimental data and other models is thus given in the next section of this paper.

4   Results and discussion

Only a few published papers were found with pH measurements at high pressure, high temperature and high salinity. None of them covered at the same time the expected validity domain of our new model. Thus, analysis of the new model capabilities could only be performed for one or two parameters at a time.

A selection of comparisons between the new model predictions and data from the literature is provided from Figure 1 to Figure 5. Comparisons with other models freely available or reported in the literature were also performed. A detailed list of these models is given in Table 3. Model A refers to Corplus, which has a known validity domain consisting of 120 °C, 20 bar of CO_2 and ionic strength below 0.75 mol.L^{-1}. Model A_{fc} is a modified use of Model A, using the fugacity of CO_2 and H_2S as input instead of partial pressures (fugacity coefficients were calculated by the Soreide and Whitson's model [41]). Model B was taken from a paper by Duan and Sun [51] with an approach based on Pitzer's theory and an equation of state for fugacity calculations, very similar to our new model. Model C and D consist in pH calculation models by Shell and BP respectively, with calculated values taken from [56]. Model E refers to the freely available Norsok Model [6], which can be used at temperature between 5 and 150 °C, ionic strength comprised between 0 and 3 mol.L^{-1}, and CO_2 fugacity from 0.1 to 10 bar.

Solubility predictions

Once Soreide and Whitson's model and Pitzer's model provide respectively the fugacity and activity coefficients of components in the gas phase and in the liquid phase, the Ensemble Henry's law (10) is applied to assess the solubility of H_2S and CO_2 in different conditions.
Note that in the proposed approach, we do not perform a rigorous thermodynamic flash calculation, since the fugacity equality constraint in both phases is not checked for water. It is a limitation of this approach, but the results presented further show that this approximation does not significantly affect the accuracy of the model in the considered temperature and pressure ranges.

The predictions of the new model for H_2S solubility in pure water were compared to Ng et al. [57] experimental data. These authors performed measurements of H_2S solubility in water in the case of different $CH_4/C_3H_8/H_2S/CO_2$ gas mixtures at various temperatures. Figure 1 shows the concentration of dissolved H_2S versus the total pressure of 75% CH_4–C_3H_8 (95:5 mole ratio) and 25 % H_2S–CO_2 (3:1 mole ratio). The calculation of fugacity coefficients of gases was performed assuming propane to show similar interactions properties like methane with the others components. The new model gives more accurate predictions of H_2S solubility with this set of experimental data than models A and A_{fc}.

The predictions of the new model for CO_2 solubility were compared to Rumpf et al. [58] experimental data. These authors measured CO_2 solubility in highly concentrated NaCl solutions under pressure of pure CO_2 at different temperatures. Figure 2 shows the concentration of dissolved CO_2 in 4 mol.kg^{-1} NaCl solutions versus the total pressure at 40 °C and 160 °C. On Figure 3, the prediction of the new model were also compared to another model proposed in the literature (Model B) [51] and to Takenouchi et al. experimental data [59] obtained in NaCl solutions (1 mol.L^{-1} and 4 mol.L^{-1}) at 200 °C up to 1400 bar of CO_2. The new model presents a good agreement with these solubility data, even in a highly concentrated solution and on a wide range of temperature and pressure, whereas model A presents significant error at high pressure CO_2, even after fugacity corrections (model A_{fc}). The predictions of the new model are extremely close to those obtained with Model B [51].

For highly concentrated brine solutions, these results show that the application of the ensemble Henry's law combining Dhima's constants, Soreide and Whitson's model and Pitzer's model provides accurate predictions of CO_2 and H_2S solubilities even under high temperature, high pressure. It is therefore appropriate for in-situ pH calculation, as detailed in the next part of the paper.

pH predictions

The calculation method of pH is classically derived from the electroneutrality equation as described elsewere [28]. Once H$^+$ concentration is determined, pH is calculated from H$^+$ activity according to:

$$pH = -\log a_{H^+} = -\log\left(\gamma_{H^+} \times c_{H^+}\right) \qquad (17)$$

In this expression, a_{H^+} is the activity of H$^+$, γ_{H^+} is the activity coefficient of H$^+$ and c_{H^+} is the concentration of H$^+$ in water.

Comparisons with different sets of experimental data are presented on Figure 4 and Figure 5.

Figure 4 illustrates the impact of NaCl concentration on pH. Experimental data was obtained at 25 °C and 1 bar CO_2 by Hinds et al. [56]. In the same paper, these authors compared the prediction of two models of oil and gas companies (Model C and D). The new model predicts the experimental results within less than 0.05 pH unit in the whole range of NaCl concentration from zero to more than 4 mol.L^{-1} and gives similar results to Model C and Model D. On the other hand, Model A tends to underestimate the pH value for NaCl concentration below 1 mol.L^{-1}.

Figure 5 shows pH values in pure water under CO_2 pressure up to 350 bar. Experimental data was obtained by Meyssami et al. [60] in autoclave. The new model reproduces the pH evolution with a good accuracy in all P_{CO2} domain. For comparison, calculations were also performed with Model A after fugacity correction (Model A$_{fc}$), and with the Norsok model (Model E, [6]). They both give acceptable pH values up to 50 to 100 bar CO_2.

Although no experimental data of pH measurements were found above 350 bar of acid gases, the prediction of the model was evaluated up to 2000 bar CO_2 in conditions similar to Figure 3. The results are displayed on Figure 6. It appears that above a few hundred bars of CO_2, the pH value hardly decreases, mainly due to fugacity coefficient evolution. It also appears that at constant NaCl concentration and CO_2 partial pressure, pH increases with increasing temperature. This evolution is mainly due to the decrease of CO_2 solubility at higher temperature. Finally, for the two temperature values chosen for this example i.e. 40 °C and 200 °C, we observe a different impact of NaCl concentration. At 200 °C, the calculated pH hardly varies when NaCl concentration increases from 1 to 4 mol.L^{-1}. On the contrary, at 40 °C, increasing NaCl concentration results in a significant decrease of pH, as already illustrated in Figure 4 at 25 °C.

Discussion on the validity domain

Two levels of validity domain were considered.
The first one is based only on the theoretical validity domain of the different equations used, mostly from Pitzer's model, as well as Soreide and Witson [41]. Pitzer's model was specially developed for highly concentrated electrolytes. It is thus often reported that the equations provides accurate results up to 5 to 6 mol.L^{-1} and that the equation of state for fugacity calculations is usually applicable up to 1000 bar of total pressure [61]. However, the validity domain also depends on the knowledge of Pitzer's parameters and on the accuracy of correlations chosen for equilibrium constants calculations. Considering our application, the parameters and correlations found in the literature suggest that the temperature limit is 200 °C.

The second level of validity domain which is considered is based on comparisons with experimental data. Due to the difficulty of making experiments at extremely high pressure and temperature, the range of pressure, temperature and ionic strength is narrower than the theoretical validity domain. As shown in Table 4, pH prediction of the new model could be compared with experimental data only up

to 350 bar, 42 °C and 4.25 mol.L^{-1}. Solubility prediction benefits from more published data, and the validity could thus be checked up to 1400 bar, 200 °C and 4 mol.L^{-1}.

These different validity domains are illustrated on Figure 7.

5   Conclusion

The in-situ pH of formation water is one of the most important parameters for material selection in the oil and gas production. Most prediction tools currently employed were designed in the 80s and were adapted to temperatures lower than 150 °C, maximum pressures of 50 bar and slightly concentrated solutions (up to 1 mol.L^{-1}).
However, the increasing interest of HP/HT fields requires more accurate models with extended validity domain. For this purpose, we applied a calculation method based on the ensemble Henry's law for solubility calculations and taking into account the activity of chemical species for chemical equilibrium constants calculation.
Extension of the current model used by the authors was described. It uses fugacity coefficients calculated with Soreide and Whitson's model. The effect of high concentrations of salts on the activity of chemical species in the liquid phase is modeled using Pitzer's formalism.

Even though only sparse experimental data is available in the literature at high temperature, high pressure and in concentrated solutions, all comparisons between the new model and the measurements gave a good agreement. New calculations are usually less conservative than the former ones, with higher pH values and lower H$_2$S activity. Using such models allows more accurate pH and H$_2$S fugacity predictions, with potential impacts on fit-for-purpose testing.

References

[1]   C. de Waard, D.E. Milliams, Carbonic-acid corrosion of steel, Corrosion 31 (1975) 177-181.
[2]   S. Nesic, Key issues related to modelling of internal corrosion of oil and gas pipelines - A review, Corros. Sci. 49 (2007) 4308-4338.
[3]   A. Dugstad, L. Lunde, K. Videm, Parametric study of CO$_2$ corrosion of carbon steel, Corrosion/94 paper no. 14, NACE International, Houston, TX, 1994.
[4]   A.M.K. Halvorsen, T. Sontvedt, CO$_2$ corrosion model for carbon steel including a wall shear stress model for multiphase flow and limits for production rate to avoid mesa attack, Corrosion/99 paper no. 42, NACE International, Houston, TX, 1999.
[5]   S. Nesic, J. Postlethwaite, M. Vrhovac, CO$_2$ corrosion of carbon steel - from mechanistic to empirical modelling, Corros. Rev. 15 (1997) 211-240.
[6]   NORSOK standard M-506, CO$_2$ corrosion rate calculation model, Standards Norway, Lysaker, Norway, 2005.
[7]   A. Anderko, R.D. Young, Simulation of CO$_2$/H$_2$S corrosion using thermodynamic and electrochemical models, Corrosion/99 paper no. 31, NACE International, Houston, TX, 1999.
[8]   A. Anderko, P. McKenzie, R.D. Young, Computation of rates of general corrosion using electrochemical and thermodynamic models, Corrosion 2000 paper no. 479, NACE International, Houston, TX, 2000.
[9]   A. Anderko, R.D. Young, A model for calculating the rates of general corrosion of carbon steel and 13%Cr stainless steels in CO$_2$/H$_2$S environments, Corrosion 2001 paper no. 86, NACE International, Houston, TX, .
[10]   E. Dayalan, G. Vani, J.R. Shadley, S.A. Shirazi, E.F. Rybicki, Modeling CO$_2$ corrosion of carbon steels in pipe flow, Corrosion/95 paper no. 118, NACE International, Houston, TX, 1995.

[11] E. Dayalan, F. De Moraes, J.R. Shadley, S.A. Shirazi, E.F. Rybicki, CO_2 corrosion prediction in pipe flow under $FeCO_3$ scale-forming conditions, Corrosion/98 paper no. 51, NACE International, Houston, TX, 1998.

[12] S. Nesic, J. Postlethwaite, S. Olsen, An electrochemical model for prediction of corrosion of mild steel in aqueous carbon dioxide solutions, Corrosion, 52 (1996) 280-294.

[13] S. Nesic, M. Nordsveen, R. Nyborg, A. Stangeland, A mechanistic model for carbon dioxide corrosion of mild steel in the presence of protective iron carbonate films - Part 2: A numerical experiment, Corrosion, 59 (2003) 489-497.

[14] S. Nesic, S. Wang, J. Cai, Y. Xiao, Integrated CO_2 corrosion - Multiphase flow model, Corrosion 2004 paper no. 626, NACE International, Houston, TX, 2004.

[15] S. Nesic, J. Cai, K.L.J. Lee, A multiphase flow and internal corrosion prediction model for mild steel pipelines, Corrosion 2005 paper no. 556, NACE International, Houston, TX, 2005.

[16] S. Nesic, S. Wang, H. Fang, W. Sun, K.L.J. Lee, A New updated model of CO_2/H_2S corrosion in multiphase flow, Corrosion 2008 paper no.535, NACE International, Houston, TX, 2008.

[17] M. Nordsveen, S. Nesic, R. Nyborg, A. Stangeland, A mechanistic model for carbon dioxide corrosion of mild steel in the presence of protective iron carbonate films - Part 1: Theory and verification, Corrosion, 59 (2003) 443-456.

[18] B.F.M. Pots, Mechanistic models for the prediction of CO_2 corrosion rates under multi-phase flow conditions, Corrosion/95 paper no. 137, NACE International, Houston, TX, 1995.

[19] B.F.M. Pots, R.C. John, I.J. Rippon, M.J.J.S. Thomas, S.D. Kapusta, M.M. Girgis, T. Whitham, Improvements on De Waard - Milliams corrosion prediction and applications to corrosion management, Corrosion 2002 paper no. 235, NACE International, Houston, TX, 2002.

[20] B.F.M. Pots, S.D. Kapusta, Prediction of corrosion rates of the main corrosion mechanisms in upstream applications, Corrosion 2005 paper no. 550, NACE International, Houston, TX, 2005.

[21] N. Sridhar, D.S. Dunn, A.M. Anderko, M.M. Lencka, H.U. Schutt, Effects of water and gas compositions on the internal corrosion of gas pipelines - Modeling and experimental studies, Corrosion, 57 (2001) 221-235.

[22] M.R. Bonis, J.L. Crolet, Basics of the prediction of the risks of CO_2 corrosion in oil and gas wells, Corrosion/89 paper no. 466, NACE International, Houston, TX, 1989.

[23] J.L. Crolet, M.R. Bonis, Prediction of the risks of CO_2 corrosion in oil and gas well, SPE Prod. Eng. 6 (1991) 449-453.

[24] C. de Waard, U. Lotz, Prediction of CO_2 corrosion of carbon steel, Corrosion/93 paper no. 69, NACE International, Houston, TX, 1993.

[25] C. de Waard, U. Lotz, A. Dugstad, Influence of liquid flow velocity on CO_2 corrosion: A semi-empirical model, Corrosion/95 paper no. 128, NACE International, Houston, TX, 1995.

[26] Y.M. Gunaltun, Combining research and field data for corrosion rate prediction, Corrosion/96 paper no. 27, NACE International, Houston, TX, 1996.

[27] R. Nyborg, CO_2 corrosion models for oil and gas production systems, Corrosion 2010 paper no. 371, NACE International, Houston, TX, 2010.

[28] J.L. Crolet, M.R. Bonis, pH measurements under high-pressures of CO_2 and H_2S, Mater. Performance, 23 (1984) 35-42.

[29] J.E. Oddo, M.B. Tomson, Simplified calculation of $CaCO_3$ saturation at high-temperatures and pressures in brine solutions, J. Petrol. Tech. 34 (1982) 1583-1590.

[30] D.A. Palmer, R. Van Eldik, The chemistry of metal carbonato and carbon dioxide complexes, Chem. Rev. 83 (1983) 651-731.

[31] W. Sun, Kinetics of iron carbonate and iron sulfide scale formation in CO_2/H_2S corrosion, PhD thesis, Ohio University, Athens, OH, 2006.

[32] J.J. Carroll, What is Henry's law?, Chem. Eng. Prog. 87 (1991) 48-52.

[33] J.L. Nelson, R.V. Reddy, Selecting representative laboratory test conditions for fit-for-purpose OCTG material evaluations, SPE High Pressure / High Temperature Sour Well Design Applied Technology Workshop paper no. 97576, The Woodlands, TX, 2005.

[34] M.F. Mohamed, A.M. Nor, M.F. Suhor, M. Singer, Y.S. Choi, S. Nesic, Water chemistry for corrosion prediction in high pressure CO_2 environments, Corrosion (2011) (paper no. 375).

[35] J.C. De Hemptinne, A. Dhima, S. Shakir, The Henry constant for 20 hydrocarbons, CO_2 and H_2S in water as a function of pressure and temperature, Fourteenth symposium on Thermophysical Properties, Boulder, CO, 2000.

[36] D.M. Austgen, G.T. Rochelle, C.C. Chen, Model of vapor-liquid-equilibria for aqueous acid gas-alkanolamine systems . 2. Representation of H_2S and CO_2 solubility in aqueous MDEA and CO_2 solubility in aqueous mixtures of MDEA with MEA or DEA, Ind. Eng. Chem. Res. 30 (1991) 543-555.

[37] F.J. Millero, The thermodynamics and kinetics of the hydrogen-sulfide system in natural-waters, Mar. Chem. 18 (1986) 121-147.

[38] G. Olofsson, L.G. Hepler, Thermodynamics of ionization of water over wide ranges of temperature and pressure, J. Solution Chem. 4 (1975) 127-143.

[39] C.S. Patterson, G.H. Slocum, R.H. Busey, R.E. Mesmer, Carbonate equilibria in hydrothermal systems: First ionization of carbonic acid in NaCl media to 300 °C, Geochim. Cosmochim. Acta, 46 (1982) 1653-1663.

[40] J.C. Peiper, K.S. Pitzer, Thermodynamics of aqueous carbonate solutions including mixtures of sodium-carbonate, bicarbonate, and chloride, J. Chem. Thermodyn. 14 (1982) 613-638.

[41] I. Soreide, C.H. Whitson, Peng-Robinson predictions for hydrocarbons, CO_2, N_2, and H_2S with pure water and NaCl brine, Fluid Phase Equilib. 77 (1992) 217-240.

[42] D.Y. Peng, D.B. Robinson, A new two-constant equation of state, Ind. Eng. Chem. Fundam. 15 (1976) 59-64.

[43] K.S. Pitzer, J.C. Peiper, R.H. Busey, Thermodynamic properties of aqueous sodium-chloride solutions, J. Phys. Chem. Ref. Data 13 (1984) 1-102.

[44] K.S. Pitzer, Thermodynamics of electrolytes. I. Theoretical basis and general equations, J. Phys. Chem. 77 (1973) 268-277.

[45] H.F. Holmes, R.H. Busey, J.M. Simonson, R.E. Mesmer, D.G. Archer, R.H. Wood, The enthalpy of dilution of HCl(aq) to 648 K and 40 MPa thermodynamic properties, J. Chem. Thermodyn. 19 (1987) 863-890.

[46] J.P. Greenberg, N. Moller, The prediction of mineral solubilities in natural waters: A chemical equilibrium model for the Na-K-Ca-Cl-SO_4-H_2O system to high concentration from 0 to 250 °C, Geochim. Cosmochim. Acta 53 (1989) 2503-2518.

[47] Z.H. Duan, D.D. Li, Coupled phase and aqueous species equilibrium of the H_2O-CO_2-NaCl-$CaCO_3$ system from 0 to 250 degrees C, 1 to 1000 bar with NaCl concentrations up to saturation of halite, Geochim. Cosmochim. Acta 72 (2008) 5128-5145.

[48] C.E. Harvie, N. Moller, J.H. Weare, The prediction of mineral solubilities in natural waters: The Na-K-Mg-Ca-H-Cl-SO_4-OH-HCO_3-CO_3-CO_2-H_2O system to high ionic strengths at 25 °C, Geochim. Cosmochim. Acta 48 (1984) 723-751.

[49] F. Millero, F. Huang, T. Graham, D. Pierrot, The dissociation of carbonic acid in NaCl solutions as a function of concentration and temperature, Geochim. Cosmochim. Acta 71 (2007) 46-55.

[50] R.T. Pabalan, K.S. Pitzer, Thermodynamics of NaOH(aq) in Hydrothermal Solutions, Geochim. Cosmochim. Acta 51 (1987) 829-837.

[51] Z. Duan, R. Sun, An improved model calculating CO_2 solubility in pure water and aqueous NaCl solutions from 273 to 533 K and from 0 to 2000 bar, Chem. Geol. 193 (2003) 257-271.

[52] F. Kurz, B. Rumpf, G. Maurer, Vapor-liquid-solid equilibria in the system NH_3-CO_2-H_2O from around 310 to 470 K: New experimental data and modeling, Fluid Phase Equilib. 104 (1995) 261-275.

[53] H. Carrier, Contribution à l'étude thermodynamique de solutions d'électrolytes sous haute pression, haute température, PhD thesis, Université de Pau, Pau (France), 1996.

[54] J. Xia, A. Perez-Salado Kamps, B. Rumpf, G. Maurer, Solubility of hydrogen sulfide in aqueous solutions of single strong electrolytes sodium nitrate, ammonium nitrate, and sodium hydroxide at temperatures from 313 to 393 K and total pressures up to 10 MPa, Fluid Phase Equilib. 167 (2000) 263-284.

[55] S. He, J.W. Morse, The carbonic acid system and calcite solubility in aqueous Na-K-Ca-Mg-Cl-SO_4 solutions from 0 to 90 °C, Geochim. Cosmochim. Acta 57 (1993) 3533-3554.

[56] G. Hinds, P. Cooling, A. Wain, S. Zhou, A. Turnbull, Technical note: Measurements of pH in concentrated brines, Corrosion 65 (2009) 635-702.

[57] H.-J. Ng, C.-J. Chen, H. Schroeder. Water content of natural gas systems containing acid gas, Gas Processors Association (GPA) project no. 945, research report RR-174, 2001.

[58] B. Rumpf, H. Nicolaisen, C. Ocal, G. Maurer, Solubility of carbon-dioxide in aqueous-solutions of sodium-chloride - Experimental results and correlation, J. Solution Chem. 23 (1994) 431-448.

[59] S. Takenouchi, G.C. Kennedy, The solubility of carbon dioxide in NaCl solutions at high temperatures and pressures. Am. J. Sci. 263 (1965) 445-454.

[60] B. Meyssami, M.O. Balaban, A.A. Teixeira, Prediction of pH in model systems pressurized with carbon-dioxide, Biotechnol. Progr. 8 (1992) 149-154.

[61] N. Ferrando, R. Lugo, P. Mougin, Coupling activity coefficient models, Henry constant equations, and equation of state to calculate vapor-liquid and solid-liquid equilibrium data, Chem. Eng. Process. 45 (2006) 773-782.

Figures

Figure 1: H_2S solubility in pure water versus total pressure of a 75% CH_4-C_3H_8 (95:5 mole ratio) and 25% H_2S-CO_2 (3:1 mole ratio) gas mixture at 49 °C. Comparison of the new model predictions to experimental data [57] and to Model A and fugacity-corrected Model A (Model A_{fc}).

Figure 2: CO_2 solubility in 4 mol.kg^{-1} NaCl solution versus CO_2 partial pressure at 40 °C and 160 °C. Comparison of the new model predictions to experimental data [58] and to fugacity-corrected Model A (Model A_{fc}).

Figure 3: CO_2 solubility in 1 mol.L^{-1} and 4 mol.L^{-1} NaCl solutions at 200 °C versus CO_2 partial pressure (P_{CO2}). Comparison of the new model predictions to experimental data [59], and to fugacity-corrected Model A (Model A_{fc}) and Model B [51].

Figure 4: pH versus NaCl concentration at 25 °C under 1 bar of CO_2. Comparison of the new model predictions to experimental data [56], and to Model A, Model C and Model D.

Figure 5: pH versus CO_2 partial pressure at 42 °C in pure water. Comparison of the new model predictions to experimental data [60] and to fugacity-corrected model A (Model A_{fc}) and Model E.

Figure 6: Results of pH calculations with the new model with CO_2 partial pressure at different temperature and NaCl concentration.

Figure 7: Checked domains of validity for pH and solubility predictions and acceptable application domain based on the limits of thermodynamics models.

Tables

Table 1: Parameters used for Equation (14) [35].

Acid gas i	A_i	B_i (K^{-1})	C_i (K^{-2})
H_2S	-2.25054	5.98511 x 10^3	-1.23934 x 10^6
CO_2	-6.02700 x 10^{-1}	5.85739 x 10^3	-1.23934 x 10^6

Table 2: References of Pitzer parameters used in this work.

Pitzer parameters $\beta^{(0)}$, $\beta^{(1)}$, $\beta^{(2)}$, C^{ϕ} and ψ	Reference	Validity domain
H^+ / Cl^-	[45]	273 K < T < 523 K, P < 400 bar
Ca^{2+} / Cl^-	[46]	298 K < T < 523 K
Ca^{2+} / HCO_3^-	[47]	273 < T < 523 K, P <1000 bar
Ca^{2+} / CO_3^{2-}	[47]	273 < T < 523 K, P <1000 bar
Ca^{2+} / HO^-	[48]	not reported
Na^+ / Cl^-	[43]	273 K < T < 573 K, P < 1000 bar
Na^+ / HCO_3^-	[49]	273 < T < 523 K
Na^+ / OH^-	[50]	273 K < T< 623 K, P < 400 bar
Na^+ / CO_3^{2-}	[49]	273 < T < 523 K
Cl^- / CO_2	[51]	273 K < T < 533 K, P < 2000 bar
HCO_3^- / CO_2	[52]	310 < T < 470 K
Ca^{2+} / CO_2	[47]	273 < T < 523 K, P <1000 bar
Na^+ / CO_2	[51]	273 K < T < 533 K, P < 2000 bar
Na^+ / H_2S	[53]	298 K < T < 623 K
HS^- / H_2S	[54]	313 < T < 393 K, 100 bar
H_2S / Na^+ / Cl^-	[53]	298 K < T < 623 K
Ca^{2+} / Cl^- / CO_2	[55]	T < 363 K
H_2S / Na^+ / Cl^-	[53]	298 K < T < 623 K
Ca^{2+} / Cl^- / CO_2	[55]	T < 363 K
Na^+ / Cl^- / CO_2	[51]	273 K < T < 533 K, P < 2000 bar

Table 3: Other models to which the new model was compared.

In-text designation	Usual designation, features	Claimed validity (if known)	Reference
New model	this work, using Pitzer for activity coefficients in the liquid phase and Soreide and Witson for fugacity coefficients of gqseous components.	5 to 200 °C 0 to 5 mol.L^{-1}	This work
Model A	Corplus, Total, using empirical equilibrium constants.	5 to 120 °C 0 to 20 bar CO_2 (partial pressure) 0 to 0.75 mol.L^{-1}	[22,23]
Model A$_{fc}$	Model A with the fugacity of CO_2 and H_2S gases as inputs		/
Model B	Duan and Sun model, using Pitzer for activities and Duan et al. for fugacities	0 to 350 °C 0 to 2000 bar 0 to 4.3 mol.L^{-1}	[51]
Model C	BP model	not known	[56]
Model D	Shell Model	not known	[56]
Model E	Norsok model, using empirical equilibrium constants.	5 to 150 °C 0.1 to 10 bar CO_2 (fugacity) Total pressure < 1000 bar 0 to 3 mol.L^{-1}	[6]

Table 4: Range of tested parameters in Figure 1 to Figure 5.

Figure	T (°C)	ionic strength (mol.L^{-1})	P_{CO2} (bar)	P_{H2S} (bar)	total pressure (bar)	pH
1	49	0	0 – 42	0 – 133	0 – 700	no
2	40 - 160	4	5 – 90	no	5 – 90	no
3	200	1 - 4	0 – 2000	no	0 – 2000	no
4	25	0 - 4.25	1	no	1	yes
5	42	0	0 - 350	no	0 - 350	yes
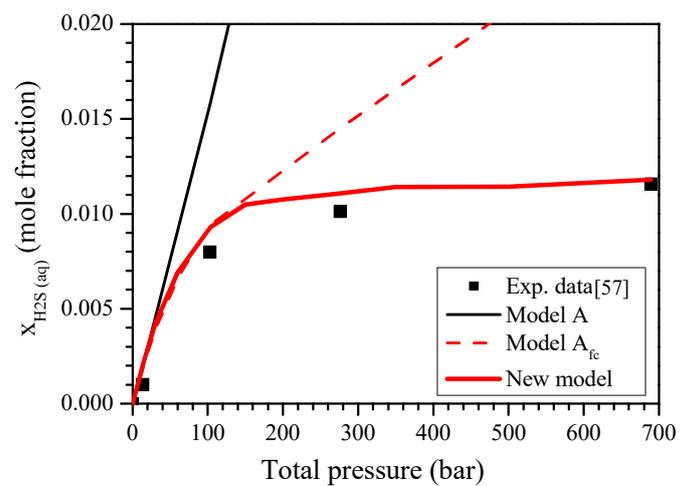
Figure

Figure 1: H₂S solubility in pure water versus total pressure of a 75% CH$_4$-C$_3$H$_8$ (95:5 mole ratio) and 25% H$_2$S-CO$_2$ (3:1 mole ratio) gas mixture at 49 °C. Comparison of the new model predictions to experimental data [57] and to Model A and fugacity-corrected model A (Model Afc).
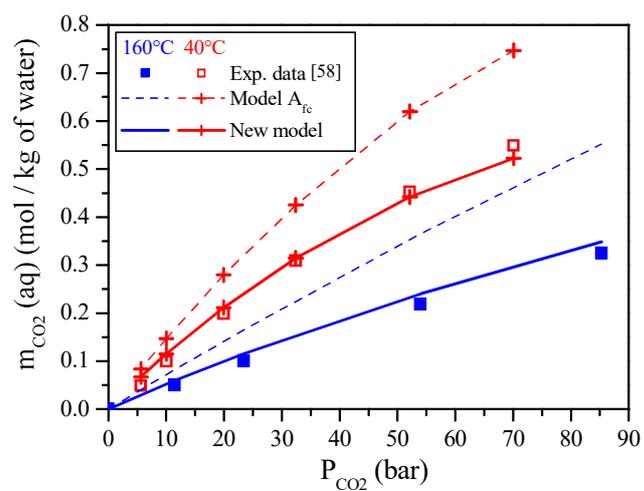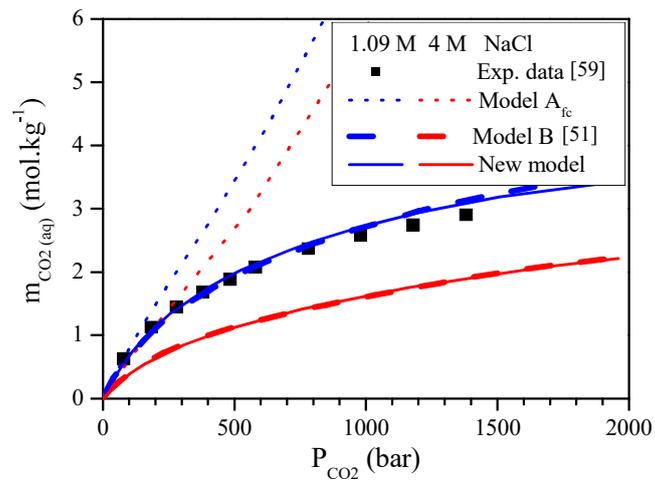
Figure 2

Figure 2: CO$_2$ solubility in 4 mol.kg^{-1} NaCl solution versus CO$_2$ partial pressure at 40 °C and 160 °C. Comparison of the new model predictions to experimental data [58] and to fugacity-corrected Model A (Model A$_{fc}$).

Figure 3

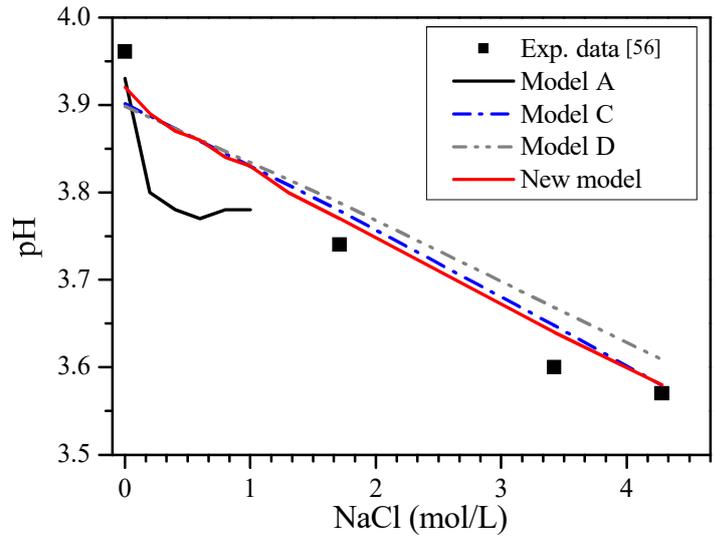**Figure 3: CO$_2$ solubility in 1 mol.L^{-1} and 4 mol.L^{-1} NaCl solutions at 200 °C versus CO$_2$ partial pressure (P$_{CO2}$). Comparison of the new model predictions to experimental data [59], and to fugacity-corrected Model A (Model A$_{fc}$) and Model B [51].**

Figure 4

Figure 4: pH versus NaCl concentration at 25 °C under 1 bar of CO_2. Comparison of the new model predictions to experimental data [56], and to Model A, Model C and Model D.
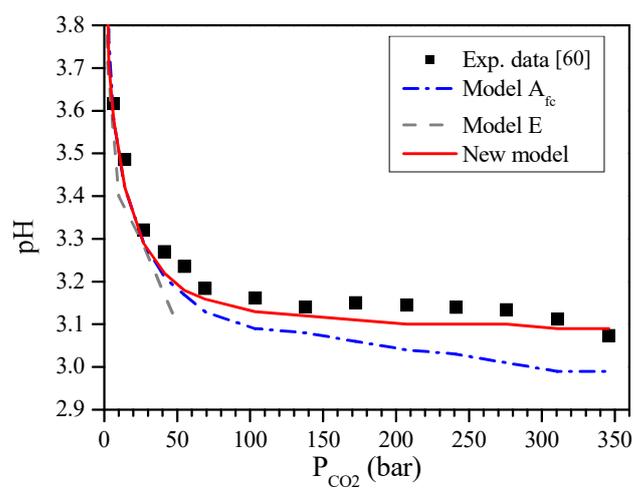
Figure 5

Figure 5: pH versus CO$_2$ partial pressure at 42 °C in pure water. Comparison of the new model predictions to experimental data [60] and to fugacity-corrected model A (Model A$_{fc}$) and Model E.
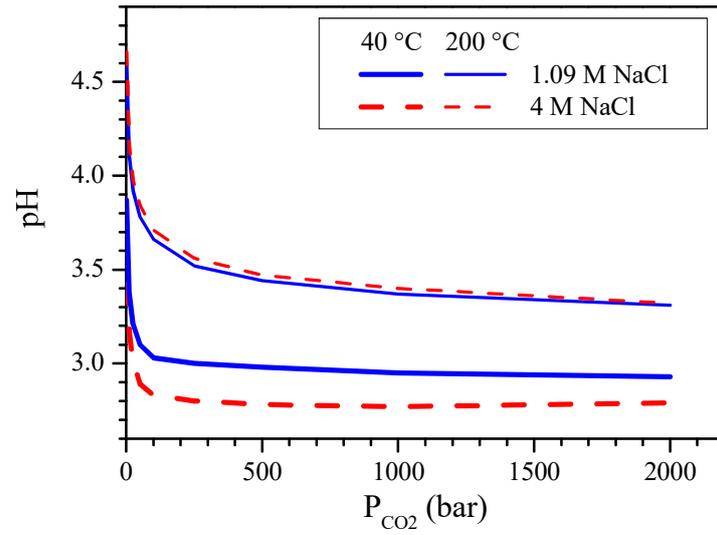
Figure 6

Figure 6: Results of pH calculations with the new model with CO$_2$ partial pressure at different temperature and NaCl concentration.
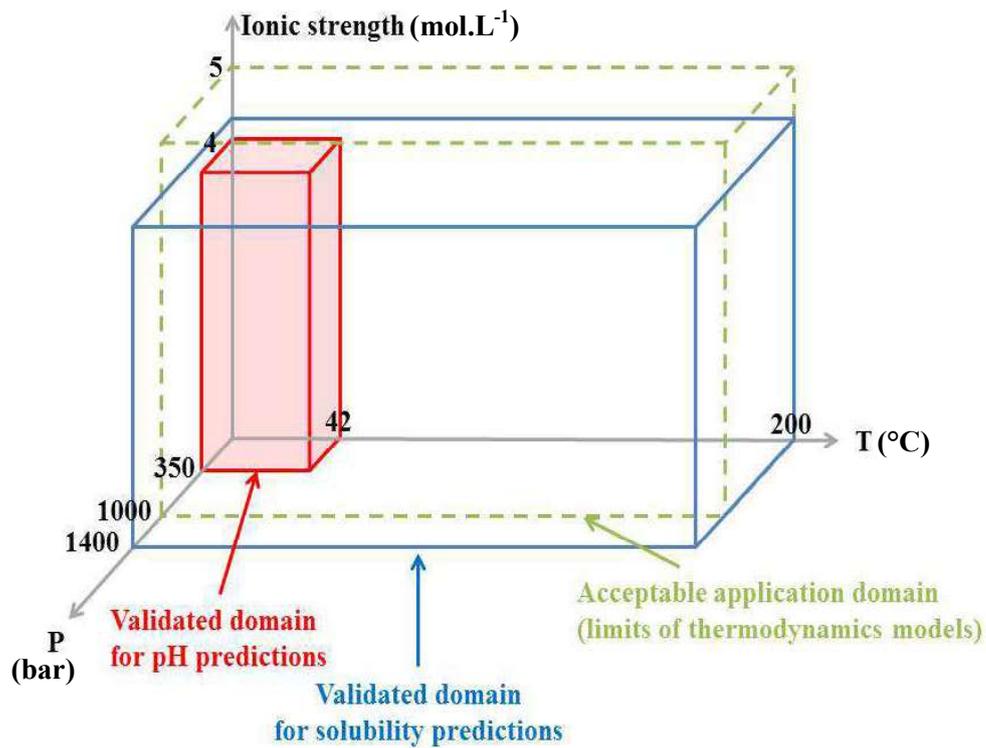
Figure 7

Figure 7: Checked domains of validity for pH and solubility predictions and acceptable application domain based on the limits of thermodynamics models.